

Plasmonic nanoring fabrication tuned to pitch: efficient, deterministic and large scale realization of ultra-small gaps for next generation plasmonic devices

D. Lehr,¹⁾ R. Alaei,²⁾ [R. Filter](#),³⁾ K. Dietrich,¹⁾ T. Siefke,¹⁾ C. Rockstuhl,^{2,4)} F. Lederer,³⁾ E.-B. Kley,¹⁾ A. Tünnermann,^{1,5)}

¹⁾*Institute of Applied Physics, Abbe Center of Photonics, Friedrich-Schiller-University Jena, Max-Wien-Platz 1, 07743 Jena, Germany*

²⁾*Institute of Theoretical Solid State Physics, Karlsruher Institut für Technologie, Wolfgang-Gaede-Str. 1, 76128 Karlsruhe, Germany*

³⁾*Institute of Condensed Matter Theory and Solid State Optics, Abbe Center of Photonics, Friedrich-Schiller-University Jena, Max-Wien-Platz 1, 07743 Jena, Germany*

⁴⁾*Institute of Nanotechnology, Karlsruher Institut für Technologie, P.O. Box 3640, 76021 Karlsruhe, Germany*

⁵⁾*Fraunhofer-Institut für Angewandte Optik und Feinmechanik IOF, Albert-Einstein-Straße 7, 07745 Jena, Germany*

A double-patterning process for scalable, efficient and deterministic nanoring array fabrication is presented. It enables gaps and features below a size of 20 nm. A writing time of 3 min per cm² makes this process extremely appealing for scientific and industrial applications. Numerical simulations are in agreement to experimentally measured optical spectra. Therefore, a platform and a design tool for upcoming next generation plasmonic devices like hybrid plasmonic quantum systems is delivered.

One of the main promises of plasmonic research has always been the possibility to enhance light-matter-interactions at the nanoscale for a large frequency range. The enormous impact of plasmonic structures on the dynamics of close-by quantum systems has been demonstrated in groundbreaking experiments¹ and new effects have been predicted². Especially the use of plasmonic structures functionalized by spectrally tunable quantum dots offers new applications in photovoltaics³, nonclassical light generation⁴, and unprecedented sensing devices⁵. However, to turn ideas into devices either scientifically or from an application perspective, it is of paramount importance to provide high-throughput reproducible fabrication processes for the plasmonic nanostructures of interest. These processes also have to cope with the extreme precision required by small feature sizes. Often, deviations of just a few nanometers in the geometry spectrally shift a resonance by hundreds of nanometers⁶. This shift would significantly degrade the ability of these plasmonic nanostructures to couple in the near-field to quantum systems that have a well-defined transition energy. With the purpose to provide a material platform that is as functional and as versatile as possible, the plasmonic properties of the nanostructures have to be deterministically scalable across an extended spectral domain.

A metallic nanostructure that has already proven its ability to serve as a strongly dispersive plasmonic building block with excellent tuning properties is a nanoring^{7,8}. Nanoring arrays can be characterized by four geometrical parameters, i.e. height, inner and outer diameter as well as period. Together with the choice of the plasmonic, substrate and filling material, nanorings offer a great tuning flexibility and a pinpoint customization capability to a broad range of applications.

In this letter, we report on a scalable and efficient multi-step process to fabricate plasmonic nanoring arrays with geometrical features and gaps below 20 nm. Utilizing character projection⁹ (CP) electron beam lithography (EBL) and a special double patterning (DP) technique allows the definition of multiple square decimeters in a reasonable timespan of hours (3 min per cm²). Thus, this process is extremely appealing for large scale fabrications. Furthermore, a cost-efficient replication is possible by nanoimprint technology¹⁰. The process is aiming for patterning of nanostructures which are characterized by small features, geometric fidelity and purity of the noble ring material.

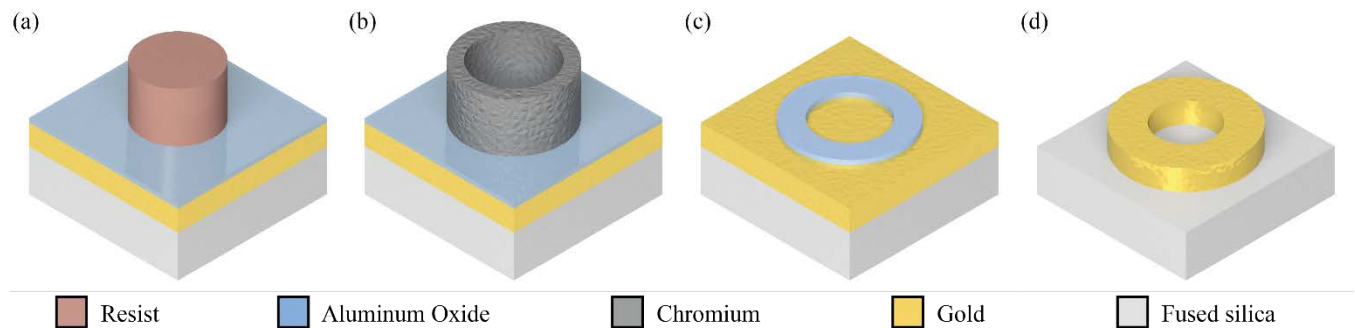


FIG. 1. Sketches of intermediate fabrication steps (see main text). (a) Template for DP, (b) chromium ring after DP, (c) Al₂O₃ ring after IBE and removal of the chromium mask & (d) gold ring after O₂-RIBE and stripping of the Al₂O₃ mask.

The fabrication process is describe as follows: Samples fabrication begins on a polished fused silica substrate. To improve the poor adhesion of gold, a 3 nm thin titanium layer is deposited by physical vapor deposition. The deposition of a 50 nm thick gold film follows subsequently in vacuum sequence. The sample is annealed at 200 °C in a furnace for 30 minutes to allow recrystallization and improvement of its plasmonic properties. Afterwards it is spin-coated with 10 nm Al₂O₃ by atomic layer deposition (ALD). In the next steps the substrate is subsequently coated with 120 nm Resist (Clariant AZ1505), covered with 10 nm chromium by ion beam deposition (IBD) and spin-coated with 110 nm chemically amplified negative tone resist (TOK CAN034). The chromium layer is primarily used as hard etching mask for the underlying photoresist AZ 1505 and secondarily as a conduction layer required for the e-beam exposure. The exposure is carried out by a Vistec SB350 OS EBL system. After development of the resist, the nanostructures were subsequently etched into the chromium layer by ion beam etching (IBE) and the AZ 1505 layer by oxygen reactive ion beam etching (O₂-RIBE). During this process, the CAN034 layer was completely removed and the template for the following self-aligned DP process¹² is achieved (Figure 1a). The template is

homogeneously coated with 30 nm chromium, i.e. angle-deposited at 45° by IBD while continuously rotating the substrate. The chromium ring is yield by removing the chromium from all horizontal surfaces and the inner resist template with IBE and oxygen plasma (Figure 1b). Fabrication is continued by transferring the chromium ring into the Al_2O_3 layer by means of IBE. Afterwards we remove the chromium ring in a NiCr solution (Figure 1c). The selectivity between Al_2O_3 and gold for O_2 -RIBE is sufficient to mask 50 nm gold with 10 nm Al_2O_3 . After transferring the Al_2O_3 mask into the gold layer by O_2 -RIBE it is wet chemically removed in phosphoric acid (Figure 1d).

Within this process, EBL is the essential limiting factor concerning the scalability for large volume fabrication, because it implies rasterization of the written sample surface. We overcome this disadvantage and partially parallelize this process by using CP, i.e. projection of a fixed mask into the resist plane. The mask contains one or more unit cells of the written pattern with a maximum area of $2.5 \mu\text{m} \times 2.5 \mu\text{m}$. By this way, the raster is increased to $2.5 \mu\text{m}$, rasterization becomes independent from the pattern, and the overall writing time can be reduced by three orders of magnitude compared to conventional EBL⁹.

Introducing an Al_2O_3 layer has multiple advantages for the whole process. First, it is a diffusion barrier between gold and chromium. Second, the etching ratio to gold and chromium is high (5:1) if oxygen is utilized as reactive etchant during IBE. Therefore, it is an etching barrier which protects the underlying gold layer from etching into it during formation of the chromium ring (Figure 2i). Later, this Al_2O_3 layer becomes an etch mask for the following gold layer. By using the low aspect ratio Al_2O_3 mask instead of the chromium ring minimizes impure re-deposition on the sidewall and broadening of the mask. The overall resolution of the etching process is increased.

The position and inner radius of the nanorings are defined by EBL. Hence, an arbitrary arrangement and inner radius of the nanorings are easily achievable within the same sample. It is for example possible to fabricate isolated nanoring dimers, trimers or structures with spatially varying geometrical properties side-by-side. The definition of all other geometrical parameters are distributed among ion beam deposition, quartz crystal controlled electron beam evaporation, ALD and (reactive) IBE with in-situ optical emission spectroscopy for end point detection. All these processes are known to be highly reproducible and accurate on the nanometer scale. In total, we expect an overall fabrication accuracy of a few nm for pattern position, thickness, height, and spacing.

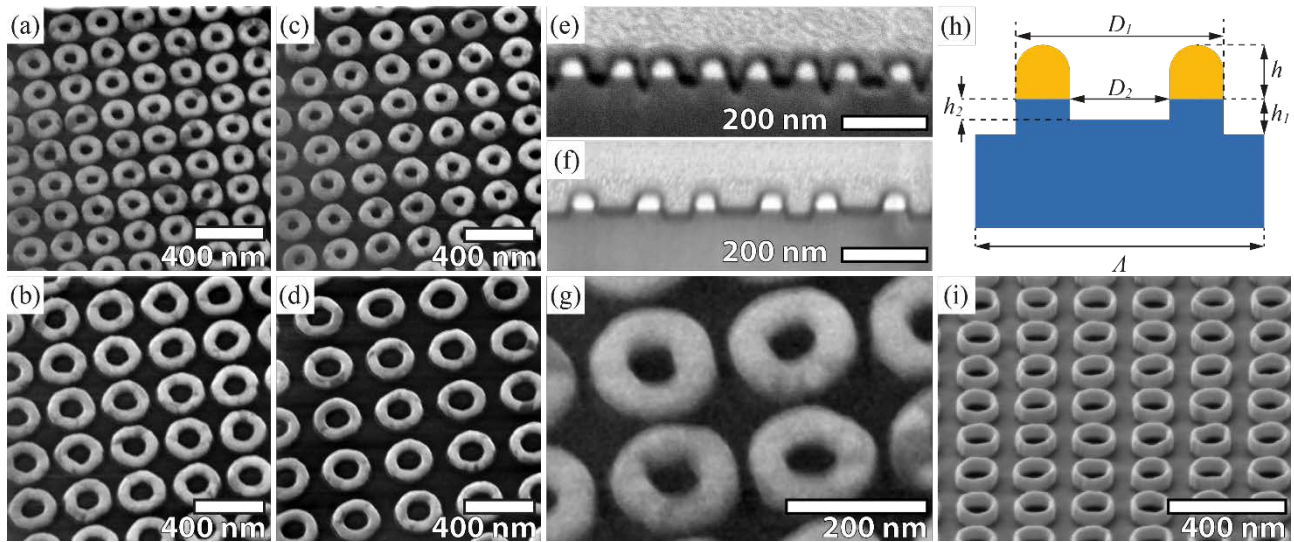


FIG. 2. Images and geometrical model of the nanoring arrays. a-d) helium ion micrographs of all 4 samples, tilted by 30°; e-f) Cross section of samples c and d; g) magnification of a; h) sketch of ring model (see measured values in Table 1); i) chromium mask of sample a tilted by 54°.

To verify this sophisticated fabrication process, we performed several experiments that serve the characterization of the fabricated samples. First, the geometry of the samples has been investigated by different imaging techniques (Figure 2). To determine the height profile, cross-sections were prepared by a Focused Gallium Ion Beam and imaged by scanning electron microscopy (SEM) (Figures 2e and 2f). The radii and distance between the nanorings were determined by evaluating helium ion micrographs (Figures 2a - 2d). This technique is superior to SEM, especially for imaging non-conducting samples¹¹. From those measurements, we derived a model of the nanorings obtained in the experiment that allows for an easy parameterization (Figure 2g). The gold ring itself is parameterized with the unit cell size Λ , the outer Diameter D_1 , the inner Diameter D_2 , and the height h . Besides the rings, the most noticeable features in the cross-sectional views (Figures 2e and 2f) are a socket at the bottom and round edges at the top side of the rings. Both properties are fully taken into account in our model. The rounding, caused by erosion of the mask edges during IBE is approximated by a radius of curvature is estimated to equal half the ring thickness $(D_1 - D_2) / 4$. The depth on the outer (h_1) and the inner (h_2) side addresses the socket, caused by poor selectivity between gold and fused silica. The measured parameters, given in Table 1, are emphasizing the flexibility and accuracy of our process. The gap and the inner diameter were tuned independently from 16 nm to 83 nm and 65 nm to 143 nm, respectively. The difference between h_1 and h_2 is most likely attributed to trenching, i.e. a localized higher etch rate near the sidewalls of a nanostructure.

Higher aspect ratio structures can be realized by increasing the thickness of the gold, chromium and aluminum oxide layers and the corresponding etching times. However, this might cause geometric shadowing while evaporating chromium under 45°. In that case, another coating technique like chemical vapor deposition or ALD should be chosen, which allows a

conformal coating. Based on the gained experience from our experiments, we assume that the features of the demonstrated structures are close to the realizable minimum with utilized tools, materials and methods. For example, a smaller separation will lead to random interconnections between adjacent rings. A smaller inner diameter will not be properly resolved by the applied electron beam resist.

TABLE I. Geometric Dimensions of the Nanoring Arrays

Λ [nm]	D_1 [nm]	D_2 [nm]	h [nm]	h_1 [nm]	h_2 [nm]	Gap [nm]
210	194	65	50	40	25	16
240	193	70	50	40	25	47
315	273	129	50	30	15	42
360	277	143	50	30	15	83
210	194	65	50	40	25	16
240	193	70	50	40	25	47
315	273	129	50	30	15	42
360	277	143	50	30	15	83
210	194	65	50	40	25	16

To evaluate the optical properties, we measured several spectra using unpolarized light in PerkinElmer Lambda 950 spectrometer and compared the results to numerical simulations (COMSOL Multiphysics®). Since the spectra are strongly depending on the geometry of the rings, their exact placement and purity of the noble metal, an agreement between measurement and simulation indicates a technological success by all parameters. Notably, an agreement will support a reliable design of future nanodevices exceeding the complexity of a periodic nanoring array. The geometry of the rings has been simulated according to the model illustrated in (Figure 2h) and described above. The permittivity of gold was taken from ellipsometric measurements of a bare layer. The comparison between experimental and numerical results is outlined in Figure 3. The plasmonic resonances of the nanoring arrays are in the near infrared region. The field inside the core of the rings is relatively homogeneous and commonly found in plasmonic nanorings⁷. By varying the period, the spectral resonance position was shifted from 750 nm to 1050 nm. Decreasing the gap between the rings leads to broadening of the resonance and a stronger field enhancement between the rings. Measurement (solid lines) and simulation (dashed lines) are in good agreement with insignificant deviations regarding the spectral resonance position, amplitude and width. Structural fluctuations and the measurement error of the geometrical dimensions only amount to few nanometers but might be accounted for those deviations. However, the overall agreement between measurement and simulation implies that impurities, which are usually introduced during etching processes, are marginal. Otherwise, we would expect a considerable red shift and broadening of the measured resonances with respect to the simulation⁸.

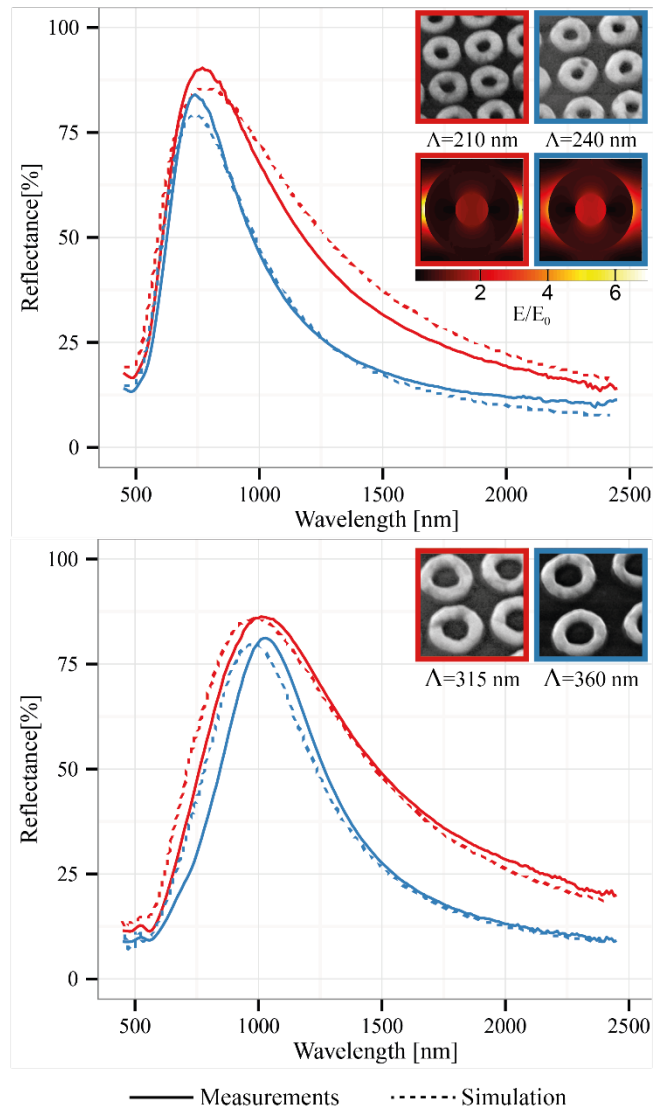


FIG. 3. Comparison of measured (solid lines) and simulated (dotted lines) reflectances for gold nanorings for different geometrical parameters. An almost perfect agreement is found in all cases. Top: periods of 210 nm (blue) and 240 nm (red) with separations of 16 nm and 47 nm, respectively. The increase in ring-to-ring distance leads to much smaller field enhancements inside the gap, see inset. Bottom: Larger periods and bigger rings lead to a huge redshift but the simple theoretical model is also applicable in this region.

In summary, we provided a reliable, deterministic and scalable double patterning process for realizing plasmonic nanorings at a writing speed of dm^2 per hours. The fabricated nanorings exhibit resonances in the near infrared regime and gaps below 20 nm. The found agreement between measurement and simulation will allow precise design of upcoming devices in future applications.

Because of the large flexibility of the geometrical parameters, the investigated nanorings offer a highly adjustable platform for next generation plasmonic devices at visual, near- and mid-infrared wavelengths. On the one hand, a gap-size down to 15 nm will allow the realization of strong coupling effects like energy splitting or level crossing if the rings are arranged as dimers⁷ or in higher order superstructures². On the other hand, the enhanced light-matter-interaction inside gaps and the

provided homogeneous field distribution inside the nanorings promise new insights and applications when combined with quantum systems to form hybrid plasmonic quantum systems.

ACKNOWLEDGMENTS

The authors gratefully acknowledge support by the German Federal Ministry of Education and Research (PhoNa 03IF2101A, OpMiSen 16SV5577) and by the Thuringian State Government (Thuringian Pro Excellence initiative, MeMa PE116-1). We also wish to thank D. Voigt, N. Sergeev, W. Gräf, M. Banasch, H. Schmidt, H.-J. Fuchs, W. Rockstroh, S. Ratzsch and T. Käsebier for their assistance during sample fabrication.

REFERENCES

- ¹O. Sqalli, M.-P. Bernal, P. Hoffmann, and F. Marquis-Weible, *Appl. Phys. Lett.* **76**, 15 (2000); D. P. Fromm, A. Sundaramurthy, P. J. Schuck, G. Kino, and W. E. Moerner, *Nano Lett.* **4**, 5 (2004); P. Mühlischlegel, H.-J. Eisler, O. J. F. Martin, B. Hecht, and D. W. Pohl, *Science* **308**, 5728 (2005); J. N. Farahani, D. W. Pohl, H.-J. Eisler, and B. Hecht, *Phys. Rev. Lett.* **95**, 1 (2005).
- ²R. Filter, S. Mühlig, T. Eichelkraut, C. Rockstuhl, and F. Lederer, *Phys. Rev. B* **86**, 3 (2012); K. Slowik, R. Filter, J. Straubel, F. Lederer, and C. Rockstuhl, *Phys. Rev. B* **88**, 19 (2013).
- ³F. Hallermann, C. Rockstuhl, S. Fahr, G. Seifert, S. Wackerow, H. Graener, G. v. Plessen, and F. Lederer, *Phys. Status Solidi A* **205**, 12 (2008); H. A. Atwater, and A. Polman, *Nat. Mater.* **9**, 3 (2010).
- ⁴J. Kim, O. Benson, H. Kan, and Y. Yamamoto, *Nature* **397**, 6719 (1999); S. Schietinger, M. Barth, T. Aichele, and O. Benson, *Nano Lett.* **9**, 4 (2009); R. Filter, K. Slowik, J. Straubel, F. Lederer, and C. Rockstuhl, *Optics Lett.* **39**, 5 (2014).
- ⁵J. L. West, and N. J. Halas, *Annu. Rev. Biomed. Eng.* **5**, 1 (2003); N. Liu, M. Mesch, T. Weiss, M. Hentschel, and H. Giessen, *Nano Lett.* **10**, 7 (2010).
- ⁶R. Alaee, C. Menzel, U. Huebner, E. Pshenay-Severin, S. B. Hasan, T. Pertsch, C. Rockstuhl, and F. Lederer, *Nano Lett.* **13**, 8 (2013).
- ⁷J. Aizpurua, P. Hanarp, D. S. Sutherland, M. Käll, Garnett W. Bryant, and F. J. García de Abajo, *Phys. Rev. Lett.* **90**, 5 (2003); P. Nordlander, *ACS Nano* **3**, 3 (2009); S. Kurth, K. Hiller, N. Neumann, M. Seifert, M. Ebermann, J. Zajadacz, and T. Gessner, *Proc. SPIE* **7713**, 77131S (2010); J. Ye, M. Shioi, K. Lodewijks, L. Lagae, T. Kawamura, and P. van Dorpe, *Appl. Phys. Lett.* **97**, 16 (2010); M. Toma, K. Cho, J. B. Wood, and R. M. Corn, *Plasmonics* **9**, 4 (2013); R. Near, C. Tabor, J. Duan, R. Pachter, and M. El-Sayed, *Nano Lett.* **12**, 4 (2012); C.-Y. Tsai, J.-W. Lin, C.-Y. Wu, P.-T. Lin, T.-W. Lu, and P.-T. Lee, *Nano Lett.* **12**, 3 (2012).
- ⁸D. Lehr, K. Dietrich, C. Helgert, T. Käsebier, H.-J. Fuchs, A. Tünnermann, and E.-B. Kley, *Opt. Lett.* **37**, 2 (2012).
- ⁹E.-B. Kley, U. Zeitner, M. Banasch, and B. Schnabel, *Proc. SPIE* **8352** (2012); K. Dietrich, D. Lehr, C. Helgert, A. Tünnermann, and E.-B. Kley, *Adv. Mater.* **24**, 44 (2012); K. Dietrich, C. Menzel, D. Lehr, O. Puffky, U. Hübner, T. Pertsch, A. Tünnermann, and E.-B. Kley, *Appl. Phys. Lett.* **104**, 19 (2014); E.-B. Kley, and U. Zeitner, *Proc. SPIE* **6290** (2006);
- ⁹A. Cattoni, E. Cambril, D. Decanini, G. Faini, and A. Haghiri-Gosnet, *Microelectron. Eng.* **87**, 5 (2010).
- ¹⁰L. Scipioni, C. A. Sanford, J. Notte, B. Thompson, and S. McVey, *J. Vac. Sci. Technol.* **27**, 6 (2009).

¹²P. Zimmerman, *Double patterning lithography: double the trouble or double the fun?*, SPIE Newsroom (2009), DOI: 10.1117/2.1200906.1691